



HAL
open science

Energy depletion by cell proliferation sensitizes the kidney epithelial cells to injury

Pierre Galichon, Morgane Lannoy, Li Li, Justine Serre, Sophie Vandermeersch, David Legouis, M Todd Valerius, Juliette Hadchouel, Joseph V Bonventre

► To cite this version:

Pierre Galichon, Morgane Lannoy, Li Li, Justine Serre, Sophie Vandermeersch, et al.. Energy depletion by cell proliferation sensitizes the kidney epithelial cells to injury. *American Journal of Physiology. Renal Physiology*, 2024, 10.1152/ajprenal.00023.2023 . hal-04394815

HAL Id: hal-04394815

<https://edf.hal.science/hal-04394815>

Submitted on 15 Jan 2024

HAL is a multi-disciplinary open access archive for the deposit and dissemination of scientific research documents, whether they are published or not. The documents may come from teaching and research institutions in France or abroad, or from public or private research centers.

L'archive ouverte pluridisciplinaire **HAL**, est destinée au dépôt et à la diffusion de documents scientifiques de niveau recherche, publiés ou non, émanant des établissements d'enseignement et de recherche français ou étrangers, des laboratoires publics ou privés.

Copyright

1 RESEARCH ARTICLE

2 RUNNING HEAD: Viability of proliferating cells

3 **Energy depletion by cell proliferation sensitizes the kidney epithelial cells to injury.**

4 **Authors:** Pierre Galichon^{1,2,3*}, Morgane Lannoy², Li Li ¹, Justine Serre², Sophie Vandermeersch², David
5 Legouis⁴, M Todd Valerius¹, Juliette Hadchouel² and Joseph V Bonventre¹

6 ¹ Department of Medicine, Harvard Medical School, and Renal Division, Department of Medicine,
7 Brigham and Women's Hospital; Boston, MA, USA,

8 ² INSERM UMR_S1155, "Common and Rare and kidney diseases: from Molecular events to Precision
9 Medicine"; Paris, France,

10 ³ Sorbonne Université, APHP, AP-HP. Sorbonne Université; F-75020 Paris, France,

11 ⁴ Laboratory of Nephrology, Department of Medicine and Cell Physiology, Division of Intensive Care,
12 University Hospital of Geneva; Geneva, Switzerland,

13

14 **Author contribution:**

15 **PG:** conceptualization, data acquisition, data analysis, drafting and finalization of the manuscript

16 **ML:** data acquisition, data analysis, critical revision of the manuscript

17 **JSB:** data acquisition, data analysis, critical revision of the manuscript

18 **LL:** data acquisition, data analysis, critical revision of the manuscript

19 **SV:** data acquisition, data analysis, critical revision of the manuscript

20 **DL:** data analysis, critical revision of the manuscript

21 **MTV:** data analysis, critical revision of the manuscript

22 **JH:** data analysis, drafting and critical revision of the manuscript

23 **JVB:** conceptualization, data analysis, critical revision of the manuscript

24

25 *Correspondence: Prof Pierre Galichon
26 Inserm UMR_S1155 ; Tenon Hospital - Research Building
27 4 rue de la Chine
28 75020 Paris FRANCE
29 Phone : +33 1 56 01 76 27 ; email: pierre.galichon@aphp.fr

30

31 **Word count**

32 abstract: 196 ; text: 4422

33

34 **ABSTRACT**

35 Acute kidney injury activates both proliferative and anti-proliferative pathways, the consequences of
36 which are not fully elucidated. If an initial proliferation of the renal epithelium is necessary for the
37 successful repair, the persistence of proliferation markers is associated with the occurrence of chronic
38 kidney disease. We hypothesized that proliferation in stress conditions impacts cell viability and renal
39 outcomes. We found that proliferation is associated with cell death after various stresses in kidney
40 cells. *In vitro*, the ATP/ADP ratio oscillates reproducibly throughout the cell cycle, and cell
41 proliferation is associated with a decreased intracellular ATP/ADP ratio. *In vivo*, transcriptomic data
42 from transplanted kidneys revealed that proliferation was strongly associated with a decrease in the
43 expression of the mitochondria-encoded genes of the oxidative phosphorylation pathway, but not of
44 the nuclear-encoded ones. These observations suggest that mitochondrial function is a limiting factor
45 for energy production in proliferative kidney cells after injury. The association of increased
46 proliferation and decreased mitochondrial function was indeed associated with poor renal outcomes.
47 In summary, proliferation is an energy demanding process impairing the cellular ability to cope with
48 an injury, highlighting proliferative repair and metabolic recovery as indispensable and
49 interdependent features for successful kidney repair.

50

51 **NEW & NOTEWORTHY**

52 ATP depletion is a hallmark of acute kidney injury. Proliferation is instrumental to kidney repair. We
53 show that ATP levels vary during the cell-cycle and that proliferation sensitizes renal epithelial cells to
54 superimposed injuries *in vitro*. More proliferation and less energy production by the mitochondria are
55 associated with adverse outcomes in injured kidney allografts. This suggests that controlling the
56 timing of kidney repair might be beneficial to mitigate the extend of acute kidney injury.

57

58 **Keywords:** acute kidney injury ; cell proliferation ; energy metabolism

59

60 **INTRODUCTION**

61 Cell proliferation is essential for any life form. As the multiplication of organized structures,
62 proliferation uses energy to decrease entropy. In his book "What is Life?", Erwin Schrodinger coined
63 the term "negentropy" to define Life.(44). Thus, proliferation requires energy. It is the cornerstone not
64 only of development in multicellular organisms but also of several processes of organ repair. In the
65 presence of various stresses, however, anti-proliferative pathways are triggered, suggesting that
66 uncontrolled proliferation can be deleterious, even in non-cancerous diseases (12, 34). This is the case,
67 for example, in the context of acute kidney injury (AKI). If it is known that cell proliferation is
68 indispensable for the organ repair (37), it was also shown that alleviating cell cycle blockade by P21 or
69 P53 aggravates the course of toxic or ischemic AKI (9, 27, 32, 33, 37, 49). These observations
70 demonstrate the essential role of cell proliferation control in pathological situations.

71 A high cellular energy level is generally accepted as a marker of viability (6) and is considered
72 a prerequisite for cell proliferation (10, 60). Conversely, a persistent decrease in the level of
73 intracellular ATP is associated with cell injury and ultimately death, both in tumor and non-tumor cells
74 (26, 57). It is generally assumed that the ATP level is regulated prior to changes in proliferation (15,
75 31, 45, 47). Indeed, a low ATP level stimulates AMPK, which induces cell cycle arrest through P27,
76 P53 and P21 activation in various organs (16). By contrast, in cancer, a low ATP level is considered to
77 allow cell proliferation by stimulating aerobic glycolysis and the Warburg effect (30). Although the
78 effect of ATP variations on proliferation has been studied, the reverse mechanism, i.e. the effect of cell
79 cycle progression on the cellular energy status, is yet unexplored. Since energy depletion leads to cell
80 death (19, 57), the effect of proliferation on the energy level of the cell might critically impact cell
81 viability. In particular, we hypothesized that cell proliferation in the context of energy depletion, such
82 as an ischemic AKI, could be detrimental. We investigated the relationship between proliferation and
83 viability in human renal epithelial cells. By quantifying the ATP/ADP ratio in live cells using a single
84 cell approach, we studied the effect of proliferation on the cellular viability and characterized the
85 pattern of variation of the intracellular energy level throughout the cell cycle. Lastly, we investigated
86 how the balance between cell proliferation and energy production influences the outcomes of kidney
87 allografts. We thus identified the downregulation of mitochondrial-encoded genes of the oxidative
88 phosphorylation pathway in proliferating epithelial cells as a limiting factor for successful recovery
89 after an episode of acute kidney injury.

90

91

92 MATERIALS AND METHODS

93 Reagents are referenced in Supplemental Table S4.

94 Cell cultures

95 HK2 (ATCC® CRL-2190™) cells are immortalized male adult human renal proximal tubular cells
96 cultured at 37°C in DMEM with 10% fetal bovine serum. The live microscopy experiments were
97 conducted in Leibovitz's L-15 medium with no phenol red (Fisher, #21083027). Pharmaceutical
98 inhibitors were purchased from Selleckchem: tenovin-1 (#S8000), pifithrin-alpha (#S2929), Rigosertib
99 (#S1362) and KU-55933 (#S1092). Cell count was performed on live microscopy data using the Fiji
100 Trackmate plugin (53).

101

102 Western Blot

103 Proteins were extracted from HK2 cells with RIPA buffer containing protease and phosphatase
104 inhibitor cocktails. Total protein concentration was measured using the BCA assay (Pierce). Samples
105 were fractionated by SDS-PAGE under reducing conditions and then transferred to a nitrocellulose
106 membrane. Membranes were incubated in TBST (TBS 1X with 0.1% Tween) with the appropriate
107 primary antibodies: anti-ATP5a (Abcam ab14748), anti-MTCO1 (Abcam ab203912) and anti-HIF1a
108 (Novus NB100-449). HSC70 (Abcam, ab51052, 1:500) was used as loading control. ImageJ
109 software (National Institutes of Health) was used for quantification.

110 Viability experiments

111 Cells were grown in DMEM with 10% fetal bovine serum in the presence or absence of puromycin
112 (2µg/mL). Energy depletion was achieved in cells grown in Leibovitz's L-15 medium without glucose
113 supplementation and hypoxia obtained by applying a 100% N₂ atmosphere (ref 26700 from Air
114 products) in an airtight chamber (ref 27310 and 27311 from Stemcell) during 24h. The control cells
115 were grown in L-15 medium with 4.5 g/dL glucose supplementation under ambient atmosphere. The
116 expression of mitochondrial proteins ATP5A and MTCO1 and the induction of Hypoxia inducible factor
117 1 in hypoxic conditions were verified by western blot (Fig S1). Flow cytometry analysis for assessment
118 of dead cells was performed with the fixable viability dye Viability 405/452 Fixable Dye (Miltenyi
119 Biotec®).

120 Mitochondrial potential assay

121 Cells were grown for 24 hours in L-15 medium with 1µmol/L JC-1 (ref 65-0851-38 from Thermo
122 Fisher) under control conditions or energy depleting conditions (as described above). Mitochondria
123 were identified by the presence of JC-1 aggregates fluorescing in red, and we assessed the
124 mitochondrial potential by quantifying the red/green fluorescence ratio in mitochondria (reflecting
125 aggregates/monomers), using Fiji(42).

126 ATP/ADP ratio measurements

127 ATP and ADP measurements were performed with the ApoSENSOR ADP/ATP ratio assay (Enzo Life
128 Sciences), in accordance with the manufacturer's instructions.

129 PercevalHR was used to study the ATP/ADP ratio in live individual cells in real-time experiments,
130 spanning multiple cell cycles. Using lentiviral transformation, we generated proximal tubular cells with
131 stable expression of PercevalHR as well as pHRed, in order to adjust the PercevalHR signal on pH
132 variations(51). ATP/ADP ratio and pH were assessed by dual signal acquisition for PercevalHR (ex
133 436/495; em 540) and pHRed (ex 436/550; em 640), followed by ratiometric normalization using the
134 Ratio Plus plugin in Fiji(42). PercevalHR (ATP/ADP ratio) was further corrected for pH by normalization
135 on pHRed (51), using the Ratio Plus plugin.

136 Bioinformatic analysis

137 ATP/ADP ratio. The Fiji Trackmate plugin was used to monitor single-cell ATP/ADP ratio over time, and
138 to determine the time of cytokinesis for each cell(53). Briefly, every cell was assigned to a single
139 trajectory at a specific timepoint, with a corresponding ATP/ADP value. The times of cytokinesis were
140 noted for each cell trajectory. ATP/ADP values were represented on the y-axis as mean+/-standard
141 error, and time was represented on the x-axis in hours from either the start of the experiment or from
142 the time of cytokinesis. The full script is available as Supplemental data.

143 Computation of proliferation index, overall OXPHOS index, nuclear and mitochondrial OXPHOS index in
144 bulk RNAseq data. We then used available RNA-seq data from kidney allograft biopsies in order to test
145 the relationship between proliferation and energy metabolism *in vivo* in 163 kidney allograft biopsies
146 from 42 patients (7). The clinical and research activities being reported are consistent with the
147 Principles of the Declaration of Istanbul as outlined in the 'Declaration of Istanbul on Organ Trafficking
148 and Transplant Tourism'. We applied a previously published and validated method to compute a
149 proliferation index as the median value of a list of proliferation associated genes (56). Similarly, we
150 computed the overall OXPHOS index as the median value of the genes listed in the human OXPHOS
151 pathway of the (Kyoto Encyclopedia of Genes and Genomes database(22)). We performed the same
152 computation on the subset of mitochondria-encoded genes to obtain the mitochondrial OXPHOS
153 index. We used median value by analogy to the previously determined proliferation index, and
154 because it has the theoretical advantage over mean values of mitigating the effect of extreme values
155 in only a small subset of genes within the predefined list. However mean values correlated closely
156 ($r \geq 0.8$) with median values suggesting non-skewed expression data for the studied genes.

157 Computation of proliferation index, overall OXPHOS index, nuclear and mitochondrial OXPHOS index in
158 single-cell RNAseq data. We used the human rejecting kidney data set (61) and the Seurat package
159 from R (14, 40) to identify the different cell types (Fig. 5). We computed the proliferation index,
160 mitochondrial encoded OXPHOS and nuclear encoded OXPHOS in the epithelial cells as described for
161 bulk RNA-seq in the previous paragraph. Because the single-cell depth of sequencing is much lower
162 than for bulk RNA-seq, we used the sum of copies within the lists of genes instead of the median
163 value.

164 Pathway analysis of proliferation associated genes. We computed Kendall's tau rank correlation
165 coefficient to evaluate the correlation of every gene expression value with the proliferation index. The
166 correlations' p-values and coefficient were then processed with the LrPath web-based software
167 allowing a logistic regression pathway analysis to identify the gene sets enriched in genes with
168 proliferation-correlated expression levels. Three prespecified genesets for energy-producing
169 pathways were analyzed: "OXidative PHOSphorylation", "Tricarboxylic Acid Cycle", and "glycolysis". P-
170 values and Odds Ratios were computed as indicators of the significance and the magnitude of the
171 enrichment of these gene sets in genes with proliferation-correlated expression values.

172 Statistical analysis

173 Statistical analyses were conducted using JMP 11 (SAS). Log-transformation was performed to
174 obtain normal distribution, when necessary. Proportions, 95% confidence interval and p-values were
175 computed using the exact binomial test. Correlations were evaluated using Kendall's tau rank
176 correlation coefficient. P-values were considered significant when <0.05 . Comparison between groups
177 were considered significant when the p-value was <0.05 using a Kruskal-Wallis non-parametrical test,
178 and secondary comparisons between pairs were considered significant when the p-value was <0.05 by
179 Wilcoxon signed-rank test. Differences in ATP/ADP changes between treatment groups over time
180 were assessed by analysis of variance using a standard least square model.

181

182 RESULTS

183 Proliferating cells are more sensitive to an injury than non-proliferating ones

184 We subjected human renal epithelial cells (HK2 cell line) to a metabolic stress and compared
185 their consequences in conditions of stimulated or inhibited proliferation. HK2 cells express markers of
186 mitochondrial ATP production but are also known to be glycolytic. Thus we caused energy depletion
187 by oxygen and glucose deprivation. Oxygen deprivation was confirmed by HIF1a induction. Although
188 the expression of OXPHOS proteins remained stable in this model, it caused a decrease in
189 mitochondrial potential (Figure 1a-b and S1A), mimicking the mitochondrial dysfunction observed in
190 the injured renal tubules *in vivo* (20, 50). Proliferation was either enhanced by pifithrin- α (a P53
191 antagonist promoting G1/S and G2/M transition) or inhibited by tenovin-1 (a P53 agonist inhibiting
192 the G1/S transition) (Fig. 1c-d and S1B). . Pifithrin- α alone or tenovin-1 alone were not toxic, as they
193 did not cause cell death in the absence of puromycin. We observed that the stimulation of cell
194 proliferation promoted the death of energy-depleted cells, whereas inhibition of cell proliferation was
195 protective (Fig. 1c). Similar results were obtained when cells were exposed to puromycin, a well-
196 characterized toxicant acting through inhibition of protein synthesis (Fig1 d).

197 Taken together, these data show that proliferation enhances susceptibility to noxious stimuli
198 and/or impairs the ability of cells to survive an injury. Given that proliferation requires energy and
199 that a decreased cellular energy level results in cell death, we hypothesized that the depletion of
200 cellular energy in proliferating cells could be responsible for this enhanced susceptibility to toxic
201 influences.

203 The ATP/ADP ratio decreases when cells proliferate

204 Adenosine triphosphate (ATP) is the main energy source for intracellular processes, through its
205 cleavage into adenosine diphosphate (ADP) and hydrogen phosphate (4, 55). The intracellular

206 ATP/ADP or ATP/AMP ratio is a more reliable marker of the cellular energy status than the absolute
207 ATP concentration (8, 30). PercevalHR is a genetically encoded markers of the ATP/ADP ratio,
208 providing a reliable indicator of the intracellular energy status (2, 51). To monitor the single cell-
209 ATP/ADP ratio over time in proliferating epithelial cells, we generated human renal tubular cells (HK2
210 cell line) stably expressing PercevalHR (Fig. S2A). We first validated the quantification of the
211 ATP/ADP ratio (ATP/ADP[Perceval]) by an independent technique based on the measurement of
212 luciferin/luciferase bioluminescence (ATP/ADP[Luciferin]). The total ATP/ADP[Perceval] signal
213 correlated well with the ATP/ADP[Luciferin] ($r=0.96$, $p=0.0001$) with an intraclass correlation of 0.87.
214 We observed the expected decrease of ATP/ADP[Perceval] after chemical energy depletion with
215 blockage of glycolysis and oxidative metabolism using 2-deoxyglucose (2 DG) and sodium azide
216 (NaN_3) (Fig. S2B-C).

217 We then quantitated the single cell ATP/ADP[Perceval]. The mean ATP/ADP values over time
218 were reproducible between wells under basal conditions or during energy depletion (Fig. S2C, middle
219 panel). However, this ratio was highly variable among proliferating cells in the same well and at the
220 same time (Fig. S2C, right panel). This observation suggests that the ATP/ADP ratio is a dynamic
221 parameter, undergoing variations that are at least partly independent of the extracellular environment.
222 We hypothesized that the ATP/ADP ratio could be correlated with the cell cycle stage. To test this
223 hypothesis, PercevalHR-expressing epithelial cells were plated at various densities to achieve different
224 levels of contact inhibition of proliferation (Fig. 2A, left panel). The intracellular ATP/ADP ratio
225 increased when the cells were more confluent. To rule out a direct effect of the confluency, we cultured
226 the cells at the same densities in the presence of rigosertib, a potent polo-like-kinase 1 (PLK1) inhibitor
227 inducing G2/M arrest. Non-proliferating cells showed a significant increase in the ATP/ADP ratio,
228 regardless of their degree of confluence. Conversely, performing a scratch assay on confluent cells

229 induced the proliferation and migration of the cells, which then displayed a low ATP/ADP ratio (Fig.
230 2A, right panel). Rigosertib increased the cellular ATP/ADP ratio while inhibiting wound closure.

231 To exclude a possible cell cycle-independent effect of rigosertib, a panel of pharmaceutical
232 compounds was used to study the changes in the ATP/ADP ratio over time when the cell cycle is
233 perturbed (Fig. 2B-C). Tenovin-1 and Rigosertib were used to inhibit the cell cycle during the G1/S or
234 G2/M transition, respectively. Conversely, pifithrin- α and KU-55933 (an ATM inhibitor promoting
235 G2/M transition) were used to stimulate cell proliferation. Single-cell monitoring demonstrated that the
236 ATP/ADP ratio increased progressively over time when cell proliferation was inhibited whereas it
237 decreased when cell proliferation was stimulated (Fig. 2C).

238

239 Cell cycle and proliferation-dependent variations in the intracellular ATP/ADP ratio

240 We then followed the variation of single-cell ATP/ADP ratio throughout the cell cycle. We thus
241 observed that the ratio was maximal around cytokinesis (Fig. 3A, left panel). This analysis was
242 performed using single cell tracking in non-synchronized cells, ruling out an effect of time or an effect
243 of the extracellular environment and suggesting a direct association with the cell cycle stage. Variations
244 of the ATP/ADP ratio before and after cytokinesis follow a systematic pattern (Fig. 3A, right panel):
245 after a gradual increase, the ratio peaks at mitosis before dropping dramatically. This pattern was
246 highly reproducible, including in cells exposed to pharmaceutical inhibition or stimulation of the cell
247 cycle (Fig. 3B). The cell cycle inhibitor tenovin-1 increased the mean ATP/ADP ratio over time
248 compared to the cell cycle facilitator pifithrin- α (Fig. 3B). Thus, the intracellular energy level,
249 evaluated by the ATP/ADP ratio, is directly influenced by the cell cycle.

250 In order to study the variations of the ATP/ADP ratio during successive cell cycles within the
251 same cell, the trajectories of this ratio were evaluated in cells undergoing division twice in the same
252 live-imaging experiment. The cells had the same pattern of ATP/ADP variations for each of the two

253 successive mitoses. After a first mitosis, cells treated with tenovin-1 reached the second mitosis with a
254 significantly higher ATP/ADP ratio than the first mitosis, compared to cells treated with pifithrin- α , in
255 which such an increment did not occur (Fig. 3B). We conclude that cell cycle inhibition increases the
256 ATP/ADP ratio in cells independently of the cell cycle stage, in a time-dependent manner: the slower
257 the cell cycles, the more positive the cellular energy balance.

258 Association of a mitochondrial defect with proliferation in injured kidney allografts

259 The proliferation of tubular cells is indispensable for the repair of the kidney after an acute
260 injury. However, the inhibition of anti-proliferative factors such as P21 and P53 (35, 38, 49, 52) leads
261 to the aggravation of the kidney lesions and loss of function. Therefore, to test the relevance of our
262 findings in proliferating cells *in vivo*, we performed an unbiased gene enrichment analysis to identify
263 pathways associated with cell proliferation in injured kidneys by analyzing the RNA-sequencing data
264 from kidney allografts before and after transplantation by Cippa and colleagues (7). Indeed, all
265 allografts undergo an episode of acute ischemic injury between the organ procurement and the
266 transplantation into the recipient.

267 The level of proliferation was estimated using a previously published and validated proliferation
268 index, which corresponds to the median value of a list of proliferation associated genes (56). We found
269 that the KEGG items that are the most significantly associated with cell proliferation are 'Metabolic
270 pathways' (FDR: 2.87e-39) and 'Oxidative phosphorylation (OXPHOS)' (FDR: 2.94e-20). Proliferation
271 and the expression level of OXPHOS genes of the pathway were negatively correlated in kidney
272 allografts immediately after transplantation (Fig. 4A and Tables S1 and S2). A further analysis showed
273 that this decrease in OXPHOS genes expression with proliferation was in fact due to a profound
274 downregulation of the expression of mitochondria-encoded genes. In contrast, the transcription of the
275 nucleus-encoded OXPHOS genes was moderately upregulated with proliferation (Fig. 4B-C, Fig. S3

276 Table S3), suggesting that mitochondrial failure is characteristic of proliferating epithelial cells in the
277 acutely injured kidney.

278 In order to verify this hypothesis at the single-cell level, we used single-cell RNA-seq data from
279 rejecting human kidneys (61) to analyze the relationship between proliferation and OXPHOS related
280 genes specifically in renal epithelial cells, identified by unsupervised analysis and verified by the
281 expression of tubular-specific markers (Fig. 5A and S4). Our analysis confirmed that proliferation was
282 negatively correlated with mitochondria-encoded OXPHOS genes, but not with nuclear-encoded
283 OXPHOS genes (Fig. 5B).

284 [Association of proliferation, mitochondrial status and outcomes.](#)

285 The study reported by Cippà and colleagues was performed on biopsies performed on the same
286 kidney allografts before, just after, 3 and 12 months after transplantation (7). The first two series of
287 samples constituted the ‘early’ group, while the last two constituted the ‘late’ group. Furthermore, three
288 types of evolution were distinguished within the late biopsies: recovery, transition towards chronic
289 kidney disease and established chronic kidney disease (CKD) (7). As shown in Fig. S5A, the computed
290 proliferation index was higher in the kidney biopsies performed 3 or 12 months after transplantation
291 than in biopsies performed immediately before or after transplantation. Moreover, a higher proliferation
292 index was associated with the progression towards CKD (Fig. S5B). OXPHOS transcripts were found
293 to be downregulated in the nucleus only during the acute phase of injury (reperfusion), whereas they
294 were downregulated in the mitochondria during the transition towards chronic kidney disease (Fig.
295 S5D, E, G,H).

296 We then studied the relationship between proliferation, the regulation of OXPHOS genes and
297 the long-term clinical outcomes, i.e. the glomerular filtration rate (GFR) and incidence of fibrosis (Fig.
298 S5C, F, I and Fig. S6). We found that the timing dramatically modified the relationship between
299 proliferation, the OXPHOS level and the incidence of fibrosis in the kidney. Although there was no

300 correlation between the proliferation index and fibrosis in the early biopsies, a low mitochondrial
301 OXPHOS index in the early biopsies (immediately before and after transplantation) was associated
302 with a lesser incidence of fibrosis in the kidney between 3 and 12 months after transplantation (Fig.
303 S5I). In contrast, a decrease in the mitochondrial OXPHOS index and an increase in the proliferation
304 index in the late biopsies (3 and 12 months after transplantation) were associated with an increased
305 fibrosis and a decreased GFR at 12 months (Fig. S5I and Fig. S6).

306 Taken together, these transcriptomic analyses suggest that the decrease of mitochondria-encoded genes
307 represents a limiting factor for energy production by OXPHOS required for the adaptive proliferative
308 repair of the kidney allografts after injury.

309

310 DISCUSSION

311 Here we show that proliferating cells are more sensitive to injury than non-proliferating ones,
312 and that the inhibition of proliferation is protective. Proliferation causes a decrease in intracellular
313 energy with superimposed energy oscillations depending on the cell-cycle stage. *In vivo*, we found that
314 mitochondria-encoded genes were profoundly downregulated in the proliferating kidney after injury,
315 indicating mitochondrial shutdown. This is in contrast with the upregulation of nucleus-encoded genes
316 of the OXPHOS gene set (Fig. 4c). This dissociated transcriptomic pattern between mitochondrial and
317 nuclear-encoded genes suggests that the cellular energy production is limited by mitochondrial damage.
318 Finally, we found that the persistence of proliferation associated with the downregulation of
319 mitochondrial OXPHOS genes is a pattern associated with an unfavorable evolution towards chronic
320 kidney disease.

321 Proliferation and energy metabolism are interdependent

322 The fact that a low intracellular ATP induces molecular pathways downstream of AMPK to control
323 proliferation suggests the presence of a regulatory feedback to mitigate the decrease in intracellular
324 ATP levels caused by increased energy consumption. Such an effect of proliferation on ATP could
325 explain why alleviating cell cycle blockade by P21 or P53 aggravates the course of acute kidney injury
326 caused by an ischemic episode (37), and why highly proliferative tumors frequently undergo
327 spontaneous necrosis (57). The kidney energy turnover is very high. It is thus very sensitive to injury
328 (and especially ischemia), which causes an immediate decrease in energy production, overall energy
329 depletion and epithelial cell death (58). After an injury, cell proliferation is necessary to replace lost
330 cells (18). However, an increase in cell proliferation caused by the inactivation of the anti-proliferative
331 factors P53 and P21 was shown to worsen the lesions caused by an episode of ischemia-reperfusion in
332 the kidney (27, 32, 49). The p53 pathway is important to arrest the cell cycle in case of DNA damage,
333 delaying proliferation until DNA is repaired (24). Short-term blockage of p53 performed after the acute
334 phase of ischemia reperfusion may have beneficial effects on subsequent fibrosis due to a decrease in

335 the senescence-associated secretory phenotype (63) whereas earlier or continued blockade actually
336 enhances fibrosis (9)

337 DNA repair is a highly energy-demanding process fueled by mitochondrial ATP generation (39). Thus,
338 proliferation arrest might be an energy-saving mechanism, especially in an injured state. In agreement
339 with this hypothesis, we found an association between increased proliferation, ATP depletion and
340 increased cell death in renal epithelial cells in which *Nupr1* (Nuclear Protein 1) was inactivated (11).
341 *Nupr1* is a downstream effector of ATF4, a master regulator of endoplasmic reticulum stress, the
342 activation of which leads to excessive protein synthesis, causing energy depletion and cell death (13).
343 Taken together, these studies suggest that an increase in cell proliferation in conditions of stress might
344 cause critical energy depletion due to enhanced energy needs for both cell maintenance and
345 biosynthetic processes, thus resulting in cell death if a critical energy threshold is not maintained (29).
346 Ultimately if the cells do not die, they may enhance the population of DNA-damaged, cell cycle
347 arrested senescent cells and lead to fibrosis.

348 [Intercellular and intracellular variations in energy metabolism](#)

349 Our observations change the understanding of energy variations in proliferating cells (Fig. 7). Previous
350 experiments were limited by the fact that timed bulk cell analysis did not allow the study of the
351 ATP/ADP trajectories of single cells within the same extracellular environment. We show by single-
352 cell analysis that a progressive increase in the ATP/ADP ratio in proliferating cells can be observed
353 when confluence and contact inhibition increase, whereas proliferation itself (at the single-cell level) is
354 associated with a decreased ATP/ADP ratio. In addition, we show that within proliferating cells, the
355 ATP/ADP ratio oscillates with the cell cycle. These oscillations in ATP/ADP ratio are reminiscent of
356 cyclic variations of the TCA cycle flux described by Ahn and colleagues (1). This is also in keeping
357 with our *in vivo* transcriptomic data showing that nuclear OXPHOS transcripts are overexpressed in
358 proliferating cells. The intracellular energy level not only varies during the cell cycle but also depends

359 on the proliferation rate. The live monitoring in single cells demonstrates a transient physiological
360 decrease in ATP/ADP in proliferating cells.

361 [Effect of proliferation on cell viability upon injury](#)

362 In certain conditions, inhibiting proliferation might be a protective mechanism to prevent lethal energy
363 depletion in epithelial cells or prevent propagation of cells with damaged DNA. This mechanism might
364 be responsible for the protective effect of the extensively studied phenomenon of ischemic
365 preconditioning (3, 5, 28), where a mild and transient ischemia triggers cytoprotective pathways
366 concomitant with transient cell cycle arrest (35, 41). Among these pathways, p53, p21 and AMPK were
367 shown to protect the kidneys from the early lesions induced by ischemia-reperfusion injury while
368 suppressing cell proliferation (21, 34).

369 However, cell proliferation is absolutely necessary for vital processes. Following a renal
370 epithelial injury, epithelial proliferation is known to be instrumental to organ repair (18). Proliferation
371 demands a high energetic input, and oxidative phosphorylation is the most efficient pathway for energy
372 production. In keeping with that, we found that proliferation is associated with increased expression of
373 nucleus-encoded OXPHOS genes in injured kidneys. Kidneys transitioning to fibrotic chronic kidney
374 disease display a dissociated transcriptomic pattern: high proliferation index with maintained
375 expression of nucleus-encoded OXPHOS genes but decreased expression of mitochondria-encoded
376 OXPHOS genes. This mitochondrial imbalance is known to be deleterious (48). In vitro, hypoxia and
377 glucose deprivation did decrease mitochondrial potential, and caused cell death in proliferating cells,
378 without causing mitonuclear imbalance, suggesting proliferating cells are sensitive to mitochondrial
379 dysfunction in general (Figure S1). This is in keeping with recent studies showing that maintaining
380 oxidative phosphorylation during and after acute kidney injury (AKI) is protective (23, 36, 54). Other
381 studies also suggested that energy-parsimonious approaches might mitigate renal damage at the early
382 stage of acute kidney injury. For example, the stabilization of the hypoxia inducible factor (HIF) shifts

383 the energy metabolism to anaerobic glycolysis, inhibits cell proliferation (12, 17, 25) and protects
384 against ischemic acute kidney injury (43, 46, 59).

385 Proliferation as a therapeutic target in kidney diseases

386 We identified kidney epithelial proliferation as a state of energy crisis with increased sensitivity to cell
387 death. However, epithelial cell proliferation is necessary for kidney repair. Thus, an interesting strategy
388 to mitigate necrosis would be to delay proliferative repair in kidneys with ongoing injury, and allow
389 proliferation after cessation of the injury. However, identifying the optimal time frame for the
390 inhibition of proliferation after kidney injury in individual patients will necessitate the implementation
391 of dynamic biomarkers of acute kidney injury. In this perspective, the cell cycle arrest markers IGFB7
392 and TIMP2 are clinically available urinary markers that might help to refine the different stages of
393 injury and repair after acute kidney injury (62). Urinary quinolate/tryptophan ratio is another
394 emerging non-invasive marker allowing to pinpoint the mitochondrial defect during acute kidney injury
395 (36).

396 Targeting the cell cycle to orchestrate kidney repair is an attractive option, but raises the concern of
397 extrarenal side effects, as proliferation is both necessary for the self-renewal of certain tissues like gut
398 or blood cells, and also instrumental in the development of cancers. Thus, targeting proliferation in a
399 time and tissue specific manner would be an advantageous strategy to improve renal outcomes while
400 minimizing the risk of side effects.

401

402 **PERSPECTIVES AND SIGNIFICANCE**

403 Proliferation is an energy demanding process impairing the cellular ability to cope with a toxic or
404 ischemic injury. We postulate that interventions to mitigate proliferation and restore energy production
405 can enhance cell survival and organ recovery (Fig. 7).

406

407 **SUPPLEMENTAL MATERIAL:**
408 <https://doi.org/10.6084/m9.figshare.24504028>

409
410 **Fig. S1. A.** Expression of HIF1alpha, ATP5A and MTCO1. **B.** Proliferation in cells incubated with
411 vehicle, Pifithrin alpha or tenovin-1, represented as relative cell count per field.

412 **Fig. S2.** Monitoring of intracellular ATP/ADP ratio.

413 **Fig. S3.** Transcriptomic signature associated with proliferation at different time points of kidney
414 transplantation.

415 **Fig. S4.** Proliferation index and renal epithelial cell differentiation markers in single cells from a
416 rejecting human kidney.

417 **Fig. S5.** Association of proliferation index and OXPHOS with chronic kidney disease progression.

418 **Fig. S6.** Association of the proliferation index and the OXPHOS indexes with long term outcomes.

419 **Table S1.** Association of proliferation-associated genes with energy metabolism pathways from the
420 KEGG encyclopedia.

421 **Table S2.** Metabolic pathways and genes associated with proliferation in injured kidneys (reperfusion).

422 **Table S4.** Key resources.

423 **Data File S1.** Fiji Jython script for single cell ratiometric analysis

424 **Movie S1.** Live PercevalHR video: scratch assay.

425 **Movie S2.** Live PercevalHR video: effect of various cell-cycle acting molecules.

426

427

428 **DISCLOSURE:**

429 Authors declare that they have no competing interests.

430 **GRANTS:**

431 Institut National de la Santé et de la Recherche Médicale ATIP Avenir program (PG)

432 Monahan Foundation (PG)

433 Fondation pour la Recherche Médicale (PG)

434 Groupe Pasteur Mutualité (PG)

435 Société Francophone de Transplantation (PG)

436 Société Francophone de Néphrologie, Dialyse et Transplantation (PG)

437 Arthur Sachs fellowship (PG)

438 Philippe Foundation (PG)

439 Fulbright Scholarship (PG)

440 Fondation de l'Avenir (PG)

441 National Institute of Health/National Institute of Diabetes and Digestive and Kidney Diseases
442 2R01DK072381 (JVB)

443 National Institute of Health/ National Institute of Diabetes and Digestive and Kidney Diseases
444 R37DK039773(JVB)

445 National Institute of Health/ National Institute of Diabetes and Digestive and Kidney Diseases
446 UH3 TR002155 (JVB)

447

448

449

450

452 **REFERENCES**

- 453 1. **Ahn E, Kumar P, Mukha D, Tzur A, Shlomi T.** Temporal fluxomics reveals oscillations in
454 TCA cycle flux throughout the mammalian cell cycle. *Mol Syst Biol* 13:953,2017. doi:
455 10.15252/msb.20177763
- 456 2. **Berg J, Hung YP, Yellen G.** A genetically encoded fluorescent reporter of ATP:ADP ratio. *Nat*
457 *Methods* 6:161-166,2009. doi: 10.1038/nmeth.1288
- 458 3. **Bon D, Chatauret N, Giraud S, Thuillier R, Favreau F, Hauet T.** New strategies to optimize
459 kidney recovery and preservation in transplantation. *Nat Rev Nephrol* 8:339-347,2012. doi:
460 10.1038/nrneph.2012.83
- 461 4. **Bonora M, Patergnani S, Rimessi A, De Marchi E, Suski JM, Bononi A, Giorgi C, Marchi S,**
462 **Missiroli S, Poletti F, Wieckowski MR, Pinton P.** ATP synthesis and storage. *Purinergic Signal*
463 8:343-357,2012. doi: 10.1007/s11302-012-9305-8
- 464 5. **Bonventre JV.** Kidney ischemic preconditioning. *Curr Opin Nephrol Hypertens* 11:43-48,2002.
- 465 6. **Chan GK, Kleinheinz TL, Peterson D, Moffat JG.** A simple high-content cell cycle assay
466 reveals frequent discrepancies between cell number and ATP and MTS proliferation assays. *PLoS*
467 *One* 8:e63583,2013. doi: 10.1371/journal.pone.0063583
- 468 7. **Cippà PE, Sun B, Liu J, Chen L, Naesens M, McMahon AP.** Transcriptional trajectories of
469 human kidney injury progression. *JCI Insight* 3:2018. doi: 10.1172/jci.insight.123151
- 470 8. **Crouch SP, Kozlowski R, Slater KJ, Fletcher J.** The use of ATP bioluminescence as a measure
471 of cell proliferation and cytotoxicity. *J Immunol Methods* 160:81-88,1993. doi: 10.1016/0022-
472 1759(93)90011-u
- 473 9. **Dagher PC, Mai EM, Hato T, Lee SY, Anderson MD, Karozos SC, Mang HE, Knipe NL,**
474 **Plotkin Z, Sutton TA.** The p53 inhibitor pifithrin- α can stimulate fibrosis in a rat model of
475 ischemic acute kidney injury. *Am J Physiol Renal Physiol* 302:F284-91,2012. doi:
476 10.1152/ajprenal.00317.2011
- 477 10. **Fu XF, Yao K, Du X, Li Y, Yang XY, Yu M, Li MZ, Cui QH.** PGC-1 α regulates the cell cycle
478 through ATP and ROS in CH1 cells. *J Zhejiang Univ Sci B* 17:136-146,2016. doi:
479 10.1631/jzus.B1500158
- 480 11. **Galichon P, Bataille A, Vandermeersch S, Wetzstein M, Xu-Dubois YC, Legouis D, Hertig**
481 **A, Buob D, Placier S, Bigé N, Lefevre G, Jouanneau C, Martin C, Iovanna JL, Rondeau E.**
482 Stress Response Gene Nupr1 Alleviates Cyclosporin A Nephrotoxicity In Vivo. *J Am Soc*
483 *Nephrol* 28:545-556,2017. doi: 10.1681/ASN.2015080936
- 484 12. **Gordan JD, Thompson CB, Simon MC.** HIF and c-Myc: sibling rivals for control of cancer cell
485 metabolism and proliferation. *Cancer Cell* 12:108-113,2007. doi: 10.1016/j.ccr.2007.07.006
- 486 13. **Han J, Back SH, Hur J, Lin YH, Gildersleeve R, Shan J, Yuan CL, Krokowski D, Wang S,**
487 **Hatzoglou M, Kilberg MS, Sartor MA, Kaufman RJ.** ER-stress-induced transcriptional
488 regulation increases protein synthesis leading to cell death. *Nat Cell Biol* 15:481-490,2013. doi:
489 10.1038/ncb2738
- 490 14. **Hao Y, Hao S, Andersen-Nissen E, Mauck WM, Zheng S, Butler A, Lee MJ, Wilk AJ,**
491 **Darby C, Zagar M, Hoffman P, Stoeckius M, Papalexi E, Mimitou EP, Jain J, Srivastava A,**
492 **Stuart T, Fleming LB, Yeung B, Rogers AJ, McElrath JM, Blish CA, Gottardo R, Smibert**
493 **P, Satija R.** Integrated analysis of multimodal single-cell data. *bioRxiv* 2020.10.12.335331,2020.
494 doi: 10.1101/2020.10.12.335331
- 495 15. **Hardie DG.** AMP-activated protein kinase--an energy sensor that regulates all aspects of cell
496 function. *Genes & Development* 25:1895-1908,2011. doi: 10.1101/gad.17420111
- 497 16. **Hardie DG, Ross FA, Hawley SA.** AMP-activated protein kinase: a target for drugs both ancient

- 498 and modern. *Chem Biol* 19:1222-1236,2012. doi: 10.1016/j.chembiol.2012.08.019
- 499 17. **Hubbi ME, Semenza GL.** Regulation of cell proliferation by hypoxia-inducible factors. *Am J*
500 *Physiol Cell Physiol* 309:C775-82,2015. doi: 10.1152/ajpcell.00279.2015
- 501 18. **Humphreys BD, Valerius MT, Kobayashi A, Mugford JW, Soeung S, Duffield JS,**
502 **McMahon AP, Bonventre JV.** Intrinsic Epithelial Cells Repair the Kidney after Injury. *Cell*
503 *Stem Cell* 2:284-291,2008. doi: 10.1016/j.stem.2008.01.014
- 504 19. **Izyumov DS, Avetisyan AV, Pletjushkina OY, Sakharov DV, Wirtz KW, Chernyak BV,**
505 **Skulachev VP.** Wages of fear”: transient threefold decrease in intracellular ATP level imposes
506 apoptosis. *Biochim Biophys Acta* 1658:141-147,2004. doi: 10.1016/j.bbabi.2004.05.007
- 507 20. **Jiang M, Bai M, Lei J, Xie Y, Xu S, Jia Z, Zhang A.** Mitochondrial dysfunction and the AKI-
508 to-CKD transition. *Am J Physiol Renal Physiol* 319:F1105-F1116,2020. doi:
509 10.1152/ajprenal.00285.2020
- 510 21. **Jones RG, Plas DR, Kubek S, Buzzai M, Mu J, Xu Y, Birnbaum MJ, Thompson CB.** AMP-
511 Activated Protein Kinase Induces a p53-Dependent Metabolic Checkpoint. *Molecular Cell*
512 18:283-293,2005. doi: 10.1016/j.molcel.2005.03.027
- 513 22. **Kanehisa M, Goto S.** KEGG: kyoto encyclopedia of genes and genomes. *Nucleic Acids Res*
514 28:27-30,2000. doi: 10.1093/nar/28.1.27
- 515 23. **Kang HM, Ahn SH, Choi P, Ko YA, Han SH, Chinga F, Park AS, Tao J, Sharma K,**
516 **Pullman J, Bottinger EP, Goldberg IJ, Susztak K.** Defective fatty acid oxidation in renal
517 tubular epithelial cells has a key role in kidney fibrosis development. *Nat Med* 21:37-46,2015.
518 doi: 10.1038/nm.3762
- 519 24. **Kishi S, Brooks CR, Taguchi K, Ichimura T, Mori Y, Akinfolarin A, Gupta N, Galichon P,**
520 **Elias BC, Suzuki T, Wang Q, Gewin L, Morizane R, Bonventre JV.** Proximal tubule ATR
521 regulates DNA repair to prevent maladaptive renal injury responses. *J Clin Invest* 129:4797-
522 4816,2019. doi: 10.1172/JCI122313
- 523 25. **Koshiji M, Kageyama Y, Pete EA, Horikawa I, Barrett JC, Huang LE.** HIF-1alpha induces
524 cell cycle arrest by functionally counteracting Myc. *EMBO J* 23:1949-1956,2004. doi:
525 10.1038/sj.emboj.7600196
- 526 26. **Lelli JL, Becks LL, Dabrowska MI, Hinshaw DB.** ATP converts necrosis to apoptosis in
527 oxidant-injured endothelial cells. *Free Radic Biol Med* 25:694-702,1998. doi: 10.1016/s0891-
528 5849(98)00107-5
- 529 27. **Li Y, Liu J, Li W, Brown A, Baddoo M, Li M, Carroll T, Oxburgh L, Feng Y, Saifudeen Z.**
530 p53 enables metabolic fitness and self-renewal of nephron progenitor cells. *Development*
531 142:1228-1241,2015. doi: 10.1242/dev.111617
- 532 28. **Lieberthal W, Tang M, Lusco M, Abate M, Levine JS.** Preconditioning mice with activators of
533 AMPK ameliorates ischemic acute kidney injury in vivo. *Am J Physiol Renal Physiol* 311:F731-
534 F739,2016. doi: 10.1152/ajprenal.00541.2015
- 535 29. **Lunt SY, Vander Heiden MG.** Aerobic glycolysis: meeting the metabolic requirements of cell
536 proliferation. *Annu Rev Cell Dev Biol* 27:441-464,2011. doi: 10.1146/annurev-cellbio-092910-
537 154237
- 538 30. **Maldonado EN, Lemasters JJ.** ATP/ADP ratio, the missed connection between mitochondria
539 and the Warburg effect. *Mitochondrion* 19:78-84,2014. doi: 10.1016/j.mito.2014.09.002
- 540 31. **Marcussen M, Larsen PJ.** Cell cycle-dependent regulation of cellular ATP concentration, and
541 depolymerization of the interphase microtubular network induced by elevated cellular ATP
542 concentration in whole fibroblasts. *Cell Motil Cytoskeleton* 35:94-99,1996. doi:
543 10.1002/(SICI)1097-0169(1996)35:2<94::AID-CM2>3.0.CO;2-I
- 544 32. **Megyesi J, Andrade L, Vieira JM, Safirstein RL, Price PM.** Positive effect of the induction of
545 p21WAF1/CIP1 on the course of ischemic acute renal failure. *Kidney Int* 60:2164-2172,2001.
546 doi: 10.1046/j.1523-1755.2001.00044.x

- 547 33. **Megyesi J, Price PM, Tamayo E, Safirstein RL.** The lack of a functional p21(WAF1/CIP1)
548 gene ameliorates progression to chronic renal failure. *Proc Natl Acad Sci U S A* 96:10830-
549 10835,1999.
- 550 34. **Motoshima H, Goldstein BJ, Igata M, Araki E.** AMPK and cell proliferation--AMPK as a
551 therapeutic target for atherosclerosis and cancer. *J Physiol* 574:63-71,2006. doi:
552 10.1113/jphysiol.2006.108324
- 553 35. **Nishioka S, Nakano D, Kitada K, Sofue T, Ohsaki H, Moriwaki K, Hara T, Ohmori K,**
554 **Kohno M, Nishiyama A.** The cyclin-dependent kinase inhibitor p21 is essential for the beneficial
555 effects of renal ischemic preconditioning on renal ischemia/reperfusion injury in mice. *Kidney Int*
556 85:871-879,2014. doi: 10.1038/ki.2013.496
- 557 36. **Poyan Mehr A, Tran MT, Ralto KM, Leaf DE, Washco V, Messmer J, Lerner A, Kher A,**
558 **Kim SH, Houry CC, Herzig SJ, Trovato ME, Simon-Tillaux N, Lynch MR, Thadhani RI,**
559 **Clish CB, Khabbaz KR, Rhee EP, Waikar SS, Berg AH, Parikh SM.** De novo NAD+
560 biosynthetic impairment in acute kidney injury in humans. *Nat Med* 24:1351-1359,2018. doi:
561 10.1038/s41591-018-0138-z
- 562 37. **Price PM, Megyesi J, Saf Irstein RL.** Cell cycle regulation: repair and regeneration in acute
563 renal failure. *Kidney Int* 66:509-514,2004. doi: 10.1111/j.1523-1755.2004.761_8.x
- 564 38. **Price PM, Safirstein RL, Megyesi J.** Protection of renal cells from cisplatin toxicity by cell
565 cycle inhibitors. *Am J Physiol Renal Physiol* 286:F378-84,2004. doi:
566 10.1152/ajprenal.00192.2003
- 567 39. **Qin L, Fan M, Candas D, Jiang G, Papadopoulos S, Tian L, Woloschak G, Grdina DJ, Li**
568 **JJ.** CDK1 Enhances Mitochondrial Bioenergetics for Radiation-Induced DNA Repair. *Cell Rep*
569 13:2056-2063,2015. doi: 10.1016/j.celrep.2015.11.015
- 570 40. R CT, *R: A Language and Environment for Statistical Computing.* Vienna, Austria: R Foundation
571 for Statistical Computing, 2013.
- 572 41. **Sano K, Fujigaki Y, Miyaji T, Ikegaya N, Ohishi K, Yonemura K, Hishida A.** Role of
573 apoptosis in uranyl acetate-induced acute renal failure and acquired resistance to uranyl acetate.
574 *Kidney Int* 57:1560-1570,2000. doi: 10.1046/j.1523-1755.2000.00777.x
- 575 42. **Schindelin J, Arganda-Carreras I, Frise E, Kaynig V, Longair M, Pietzsch T, Preibisch S,**
576 **Rueden C, Saalfeld S, Schmid B, Tinevez JY, White DJ, Hartenstein V, Eliceiri K,**
577 **Tomancak P, Cardona A.** Fiji: an open-source platform for biological-image analysis. *Nat*
578 *Methods* 9:676-682,2012. doi: 10.1038/nmeth.2019
- 579 43. **Schley G, Klanke B, Schodel J, Forstreuter F, Shukla D, Kurtz A, Amann K, Wiesener MS,**
580 **Rosen S, Eckardt KU, Maxwell PH, Willam C.** Hypoxia-inducible transcription factors
581 stabilization in the thick ascending limb protects against ischemic acute kidney injury. *J Am Soc*
582 *Nephrol* 22:2004-2015,2011. doi: 10.1681/ASN.2010121249
- 583 44. Schrodinger E. What is Life? In: edited by London: Cambridge University Press, 1944,
- 584 45. **Sholl-Franco A, Fragel-Madeira L, Macama AC, Linden R, Ventura AL.** ATP controls cell
585 cycle and induces proliferation in the mouse developing retina. *Int J Dev Neurosci* 28:63-
586 73,2010. doi: 10.1016/j.ijdevneu.2009.09.004
- 587 46. **Shu S, Wang Y, Zheng M, Liu Z, Cai J, Tang C, Dong Z.** Hypoxia and Hypoxia-Inducible
588 Factors in Kidney Injury and Repair. *Cells* 82019. doi: 10.3390/cells8030207
- 589 47. **Song D, Liu X, Liu R, Yang L, Zuo J, Liu W.** Connexin 43 hemichannel regulates H9c2 cell
590 proliferation by modulating intracellular ATP and [Ca²⁺]. *Acta Biochimica et Biophysica Sinica*
591 42:472-482,2010. doi: 10.1093/abbs/gmq047
- 592 48. **Soto I, Couvillion M, Hansen KG, McShane E, Moran JC, Barrientos A, Churchman LS.**
593 Balanced mitochondrial and cytosolic translomes underlie the biogenesis of human respiratory
594 complexes. *Genome Biol* 23:170,2022. doi: 10.1186/s13059-022-02732-9
- 595 49. **Sutton TA, Hato T, Mai E, Yoshimoto M, Kuehl S, Anderson M, Mang H, Plotkin Z, Chan**

- 596 **RJ, Dagher PC.** p53 is renoprotective after ischemic kidney injury by reducing inflammation. *J*
597 *Am Soc Nephrol* 24:113-124,2013. doi: 10.1681/ASN.2012050469
- 598 50. **Tang C, Dong Z.** Mitochondria in Kidney Injury: When the Power Plant Fails. *J Am Soc Nephrol*
599 27:1869-1872,2016. doi: 10.1681/ASN.2015111277
- 600 51. **Tantama M, Martínez-François JR, Mongeon R, Yellen G.** Imaging energy status in live cells
601 with a fluorescent biosensor of the intracellular ATP-to-ADP ratio. *Nat Commun* 4:2550,2013.
602 doi: 10.1038/ncomms3550
- 603 52. **Thoreen CC, Sabatini DM.** AMPK and p53 help cells through lean times. *Cell Metab* 1:287-
604 288,2005. doi: 10.1016/j.cmet.2005.04.009
- 605 53. **Tinevez JY, Perry N, Schindelin J, Hoopes GM, Reynolds GD, Laplantine E, Bednarek SY,**
606 **Shorte SL, Eliceiri KW.** TrackMate: An open and extensible platform for single-particle
607 tracking. *Methods* 115:80-90,2017. doi: 10.1016/j.ymeth.2016.09.016
- 608 54. **Tran MT, Zsengeller ZK, Berg AH, Khankin EV, Bhasin MK, Kim W, Clish CB, Stillman**
609 **IE, Karumanchi SA, Rhee EP, Parikh SM.** PGC1 α drives NAD biosynthesis linking oxidative
610 metabolism to renal protection. *Nature* 531:528-532,2016. doi: 10.1038/nature17184
- 611 55. **Veech RL, Lawson JW, Cornell NW, Krebs HA.** Cytosolic phosphorylation potential. *J Biol*
612 *Chem* 254:6538-6547,1979.
- 613 56. **Venet D, Dumont JE, Detours V.** Most random gene expression signatures are significantly
614 associated with breast cancer outcome. *PLoS Comput Biol* 7:e1002240,2011. doi:
615 10.1371/journal.pcbi.1002240
- 616 57. **Verrax J, Dejeans N, Sid B, Glorieux C, Calderon PB.** Intracellular ATP levels determine cell
617 death fate of cancer cells exposed to both standard and redox chemotherapeutic agents. *Biochem*
618 *Pharmacol* 82:1540-1548,2011. doi: 10.1016/j.bcp.2011.07.102
- 619 58. **Vogt MT, Farber E.** On the molecular pathology of ischemic renal cell death. Reversible and
620 irreversible cellular and mitochondrial metabolic alterations. *Am J Pathol* 53:1-26,1968.
- 621 59. **Wang J, Biju MP, Wang MH, Haase VH, Dong Z.** Cytoprotective effects of hypoxia against
622 cisplatin-induced tubular cell apoptosis: involvement of mitochondrial inhibition and p53
623 suppression. *J Am Soc Nephrol* 17:1875-1885,2006. doi: 10.1681/ASN.2005121371
- 624 60. **Wang X, Li L, Guan R, Zhu D, Song N, Shen L.** Emodin Inhibits ATP-Induced Proliferation
625 and Migration by Suppressing P2Y Receptors in Human Lung Adenocarcinoma Cells. *Cell*
626 *Physiol Biochem* 44:1337-1351,2017. doi: 10.1159/000485495
- 627 61. **Wu H, Malone AF, Donnelly EL, Kirita Y, Uchimura K, Ramakrishnan SM, Gaut JP,**
628 **Humphreys BD.** Single-Cell Transcriptomics of a Human Kidney Allograft Biopsy Specimen
629 Defines a Diverse Inflammatory Response. *J Am Soc Nephrol* 29:2069-2080,2018. doi:
630 10.1681/ASN.2018020125
- 631 62. **Xie Y, Ankawi G, Yang B, Garzotto F, Passannante A, Breglia A, Digvijay K, Ferrari F,**
632 **Brendolan A, Raffaele B, Giavarina D, Gregori D, Ronco C.** Tissue inhibitor
633 metalloproteinase-2 (TIMP-2) • IGF-binding protein-7 (IGFBP7) levels are associated with
634 adverse outcomes in patients in the intensive care unit with acute kidney injury. *Kidney Int*
635 95:1486-1493,2019. doi: 10.1016/j.kint.2019.01.020
- 636 63. **Yang L, Besschetnova TY, Brooks CR, Shah JV, Bonventre JV.** Epithelial cell cycle arrest in
637 G2/M mediates kidney fibrosis after injury. *Nat Med* 16:535-43, 1p following 143,2010. doi:
638 10.1038/nm.2144
639
640
641
642

643 **FIGURE LEGENDS**

644

645 **Figure 1.** Consequences of cell proliferation on susceptibility to cell death. (a) Representative images
646 of JC-1 staining in control conditions (CTL) or under energy depletion (ED). The red fluorescence
647 indicates aggregates forming in high potential mitochondria. The green fluorescence indicates JC-1
648 monomers in low potential mitochondria. The composite image shows the increase in JC-1 monomers
649 under energy depletion. (b) Quantification of mitochondrial potential by JC-1 in control condition, and
650 energy depletion, showing the ratio of red/green fluorescence intensity in arbitrary units. (c) Effect of
651 cell cycle inhibition by tenovin-1 or cell cycle facilitation by pifithrin- α on cellular death caused by
652 puromycin (pre-incubation for 4 hours before puromycin exposure). (d) Effect of cell cycle inhibition
653 by tenovin-1 or cell cycle facilitation by pifithrin- α on cellular necrosis caused by energy depletion
654 (preincubation for 4 hours before oxygen and glucose deprivation). *: p-value <0.05 ; NS: statistically
655 non-significant.

656

657 **Figure 2.** Cell cycle interventions and their effects on ATP/ADP ratio. (A). Left panel: Wells were
658 plated with increasing numbers of PercevalHR expressing cells to obtain various levels of confluence
659 in control condition or with 1 μ M rigosertib to inhibit the cell cycle. Right panel: Representative
660 pictures obtained 0 and 15 hours after a scratch performed under control condition or with exposure to
661 1 μ M rigosertib to inhibit wound closure. (B) Pharmaceutical interventions on the cell cycle using
662 various compounds on PercevalHR expressing cells over an 18-hr time course (total= 7345 events):
663 KU55933 (10 μ M), pifithrin-alpha (50 μ M), rigosertib (10 μ M), tenovin-1 (10 μ M). C Quantification of
664 changes in single cell intracellular ATP/ADP ratio over an 18-hr exposure to various cell cycle
665 modifiers.

666

667 **Figure 3.** ATP/ADP variations throughout the cell cycle. (A, left panel): Live imaging on a single
668 PercevalHR expressing cell undergoing mitosis. (A, right panel): Quantification of the intracellular
669 ATP/ADP ratio in single cells during the perimitotic period with in silico synchronization on time of
670 mitosis (n= 117 mitoses). (B) ATP/ADP changes in PercevalHR expressing cells incubated with the
671 cell cycle facilitator pifithrin-alpha or with the cell cycle inhibitor tenovin-1 between 2 successive
672 mitoses (n= 42 mitoses). ATP/ADP ratio values are represented as means and whiskers indicate the
673 standard error. P-values represent the significance of the comparison between the first and second
674 mitosis within each treatment group, using a Wilcoxon signed-rank test.

675

676 **Figure 4.** Transcriptomic signature associated with proliferation. (A). KEGG pathways enrichment
677 associated with proliferation in kidney allografts immediately after reperfusion. The 20 most significant
678 pathways are labeled. (B). Vulcano plot showing the correlation between OXPPOS gene expression
679 and the computed
680 proliferation index in kidney allografts (right panel). x-axis: Kendall's k correlation coefficient; y-axis:
681 significance represented by the -log(p-value) of the correlation (Kendall); blue: mitochondria-encoded
682 genes; red: nuclear-encoded genes. (C). Differential correlations of nuclei and mitochondria-encoded
683 OXPPOS with the proliferation index in kidney allografts.

684

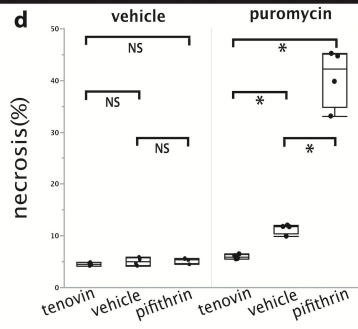
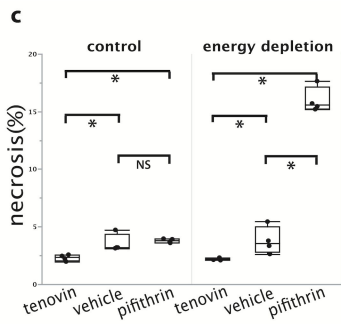
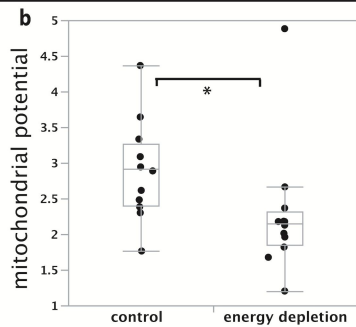
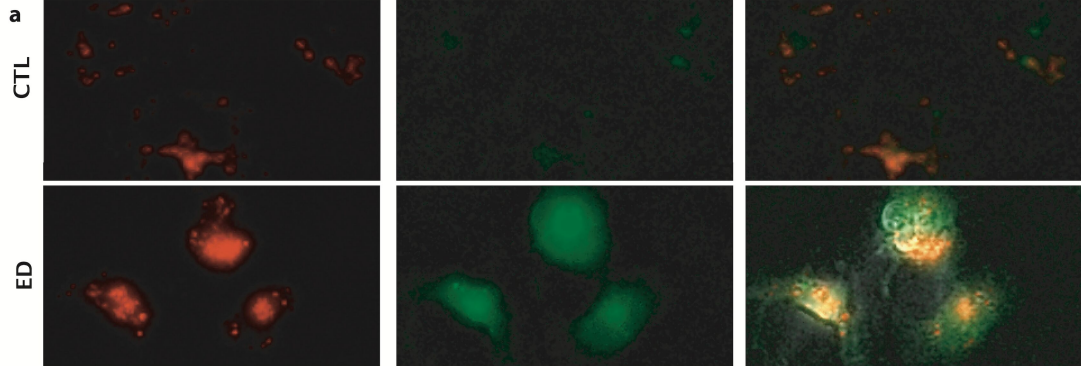
685 **Figure 5.** Oxidative phosphorylation in proliferating epithelial cells. (A) Single-cell RNA-seq analysis
686 of human rejecting kidney showing clusters corresponding to different cell types within the kidney. The
687 subset of epithelial cells is circled in red. (B) In the subset of renal epithelial cells (PT, LOH and CD),
688 an increased proliferation correlated with a decreased expression of mitochondria-encoded OXPPOS
689 genes (mean values of oxphos gene expression with standard-error whiskers, by proliferation index
690 values rounded to the nearest 10^{-5}).

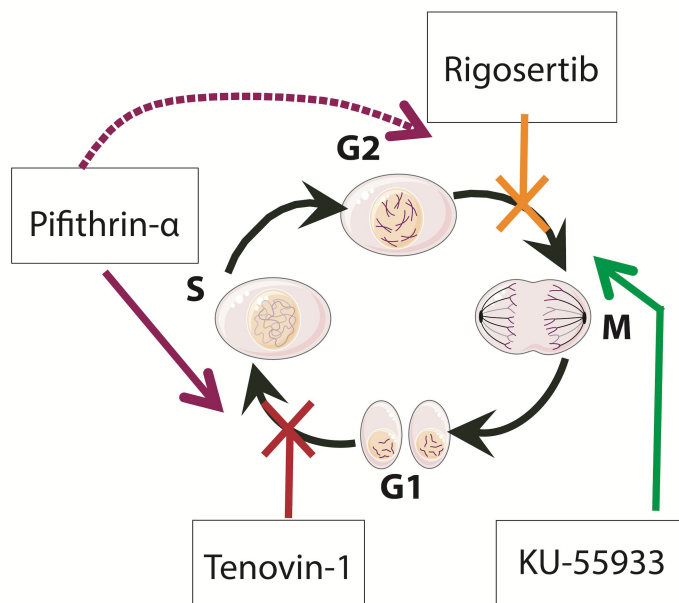
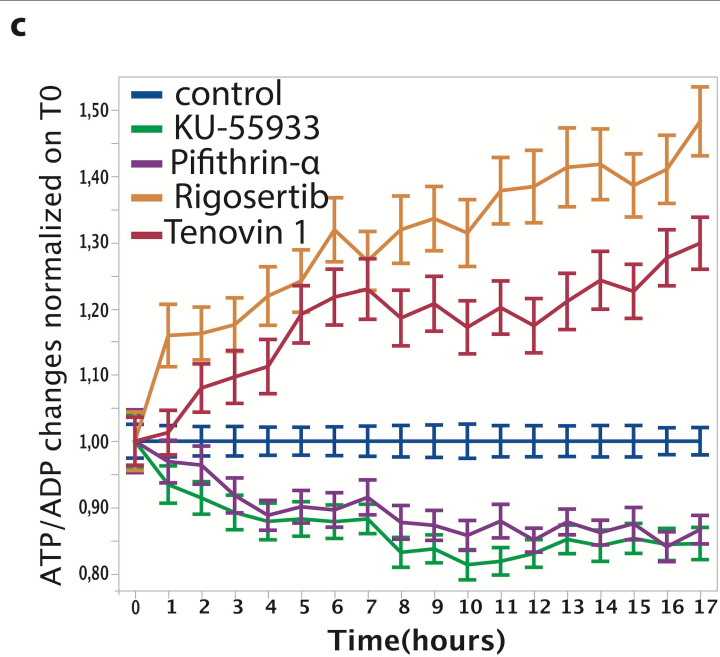
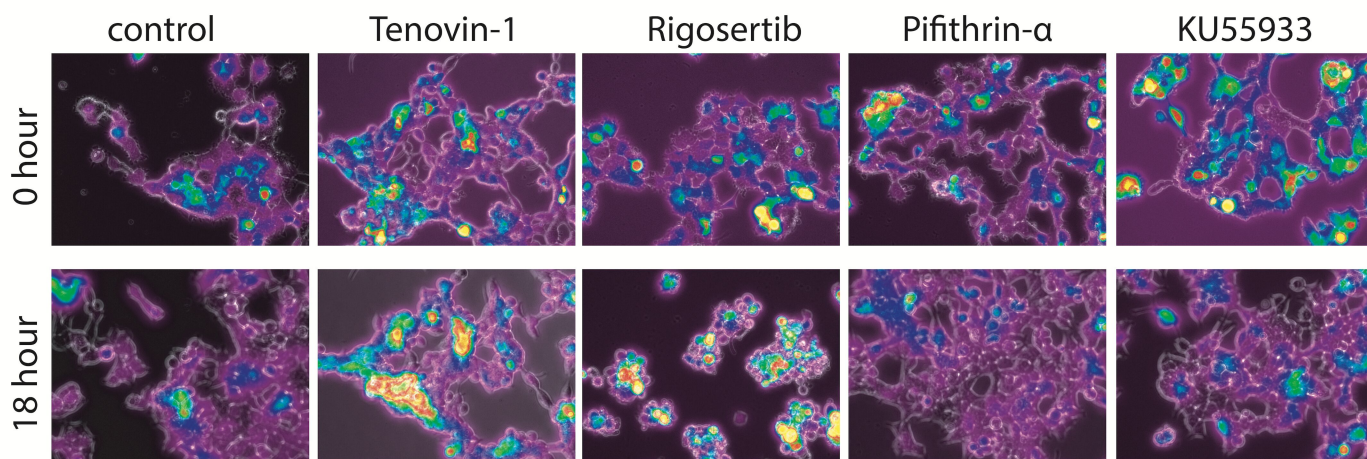
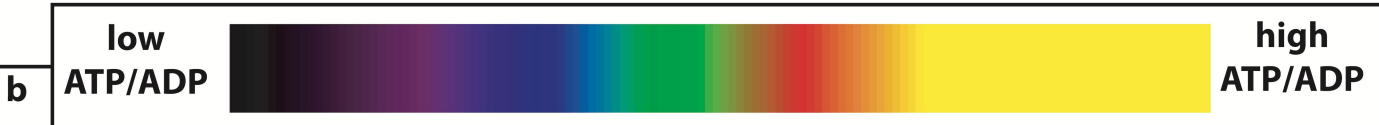
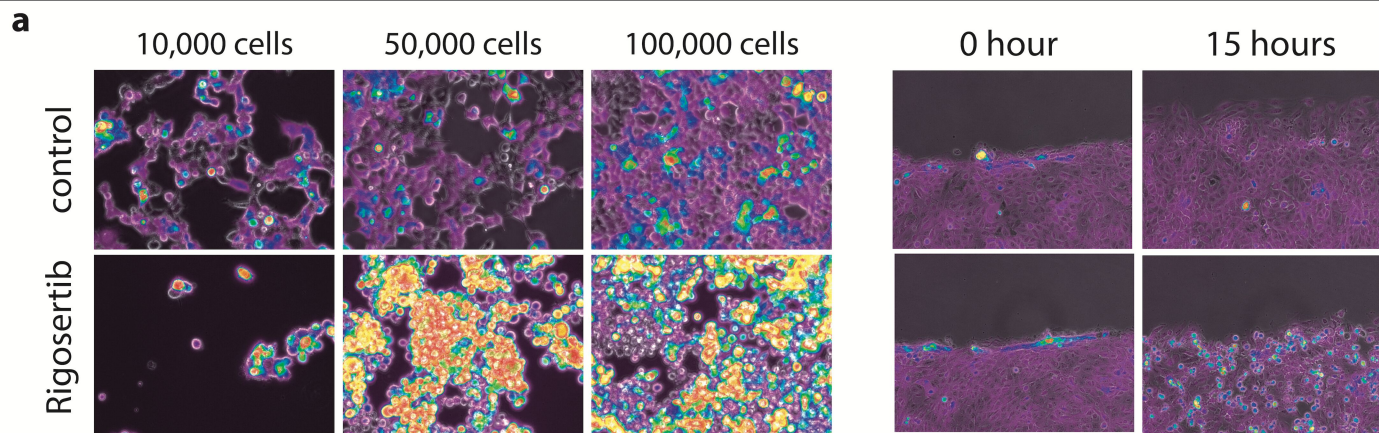
691

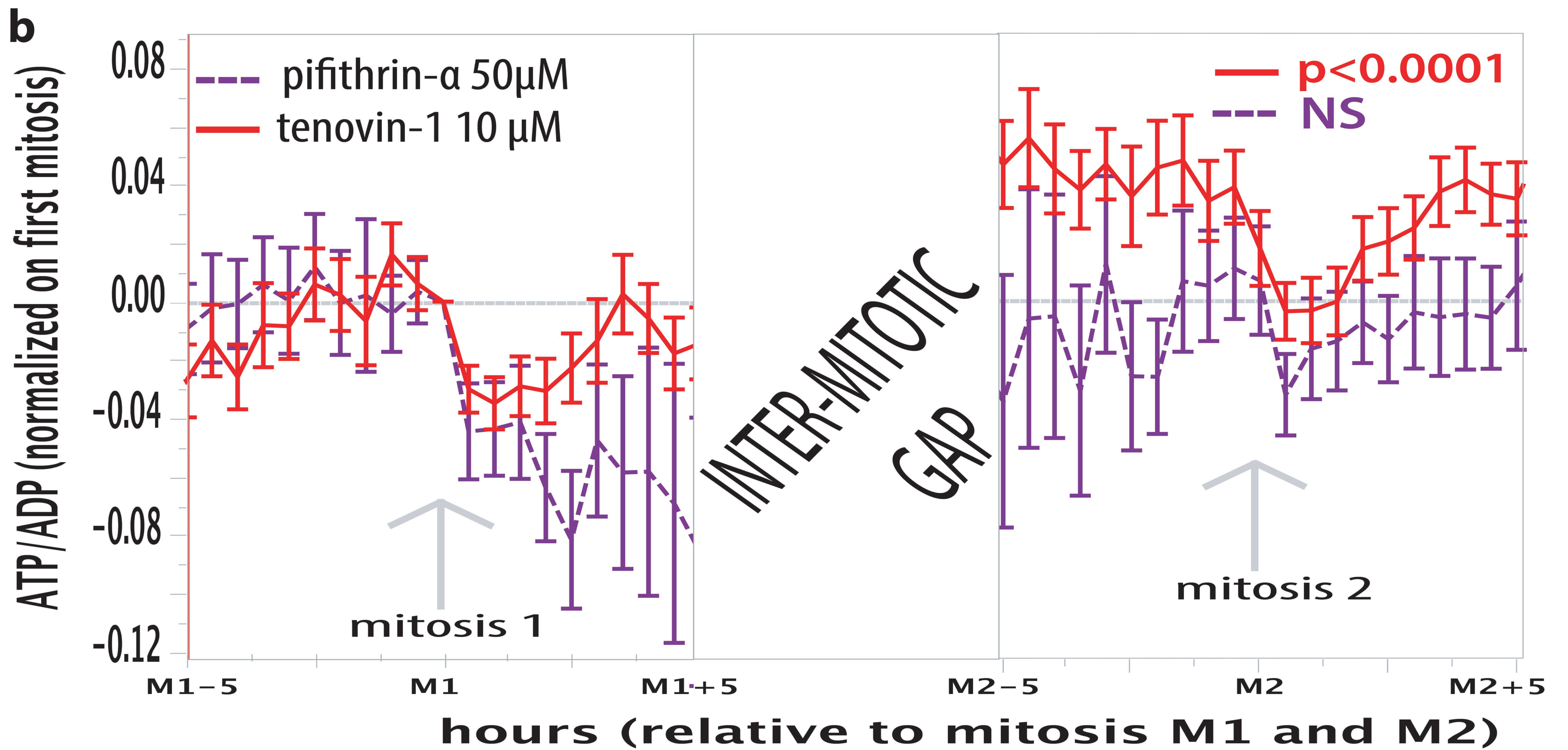
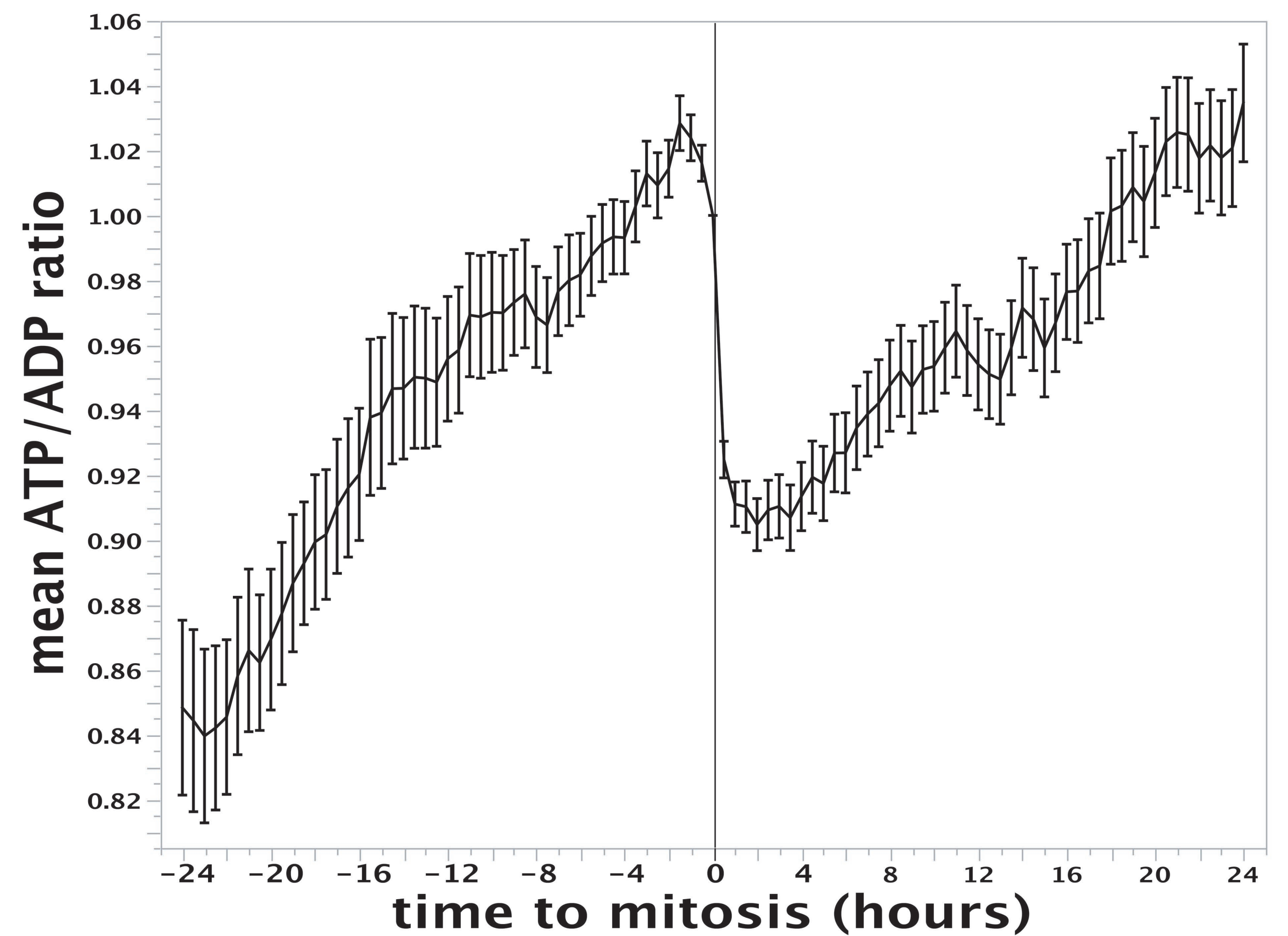
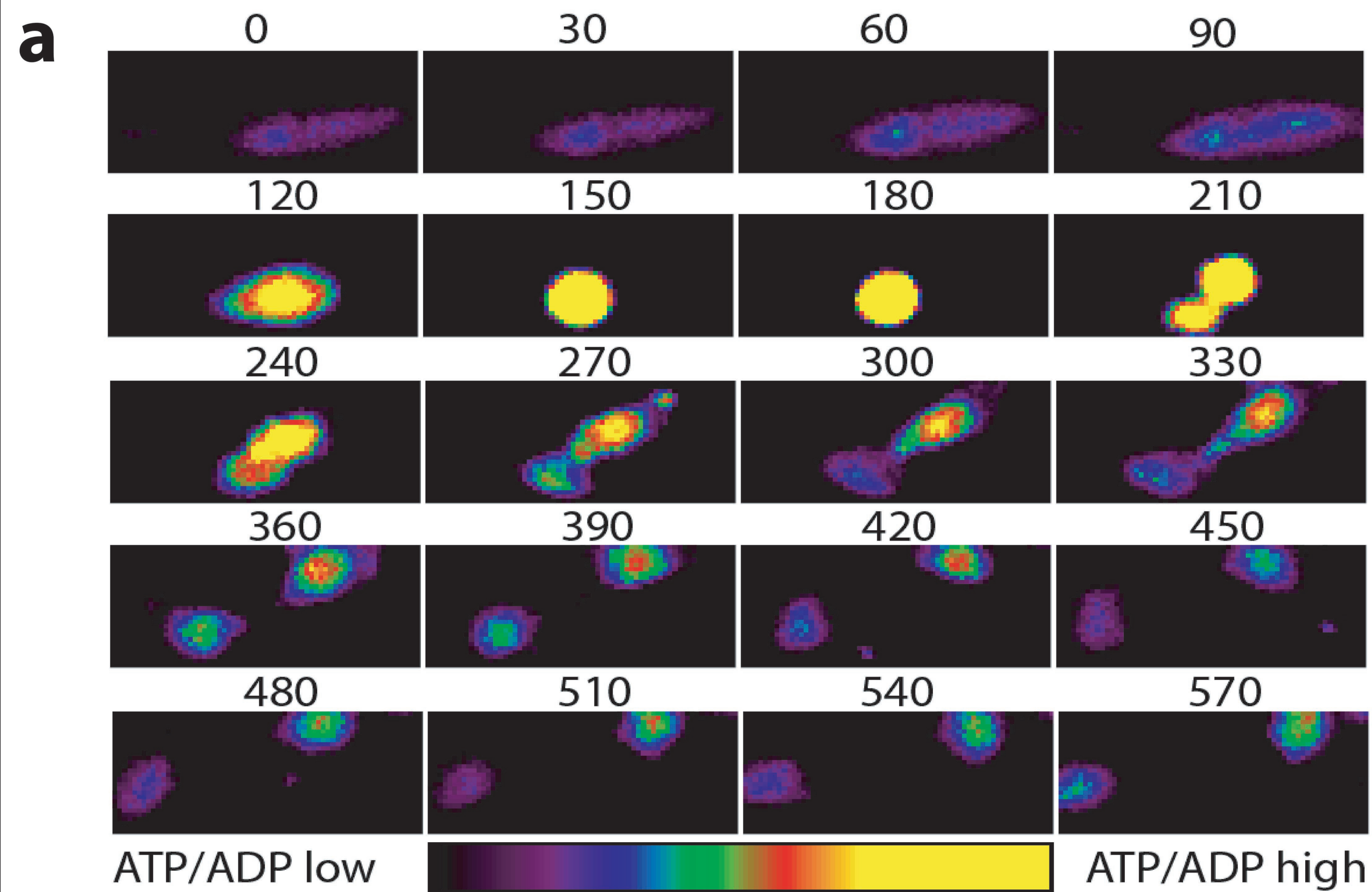
692 **Figure 6.** Association of proliferation index and OXPHOS mitochondrial genes expression with
693 chronic kidney disease progression. (A) Expression of nucleus-encoded OXPHOS genes was not
694 correlated with proliferation index or evolution towards chronic kidney disease. (B) Expression of
695 mitochondria-encoded OXPHOS genes was strongly correlated with proliferation index and evolution
696 towards chronic kidney disease.

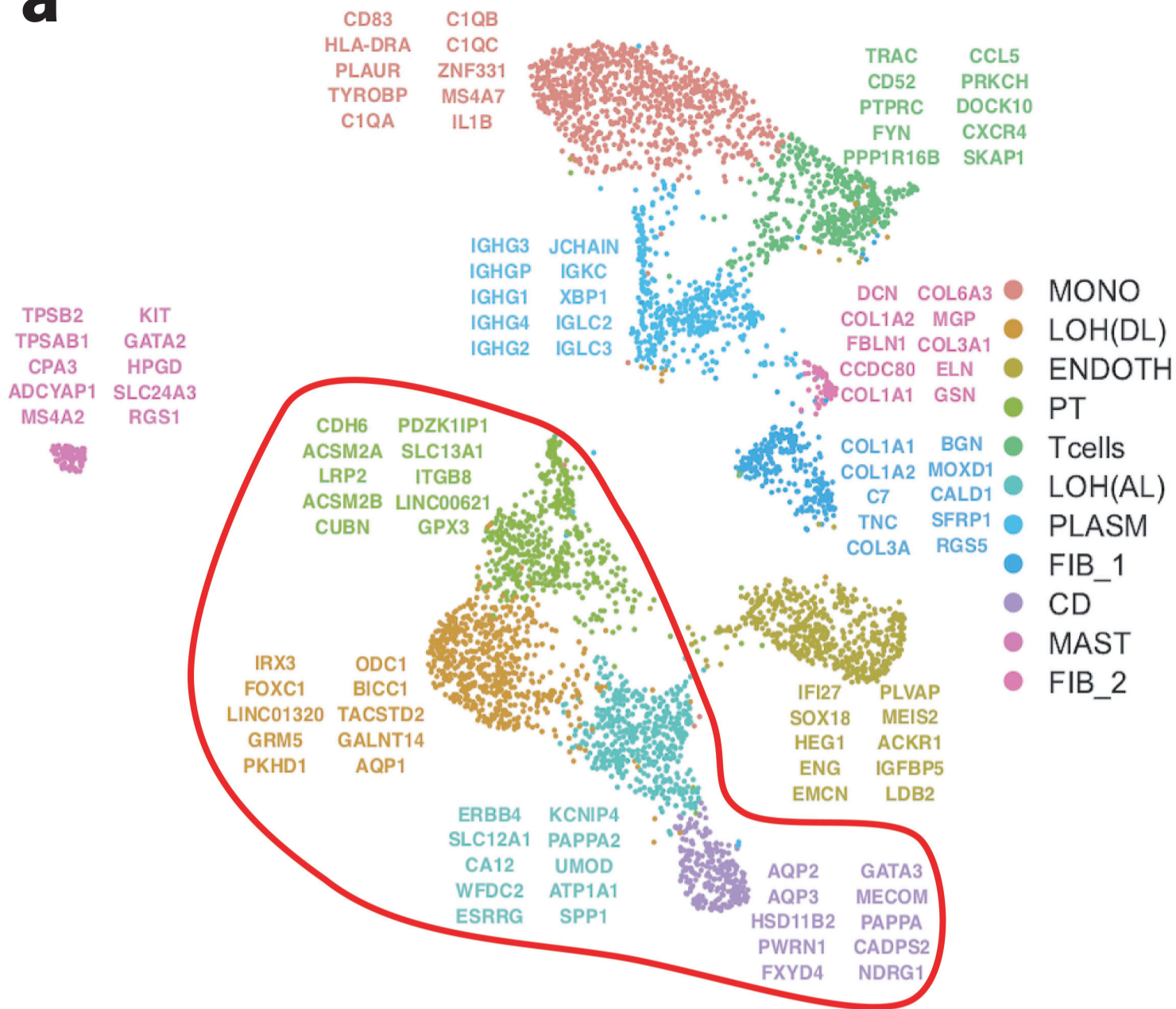
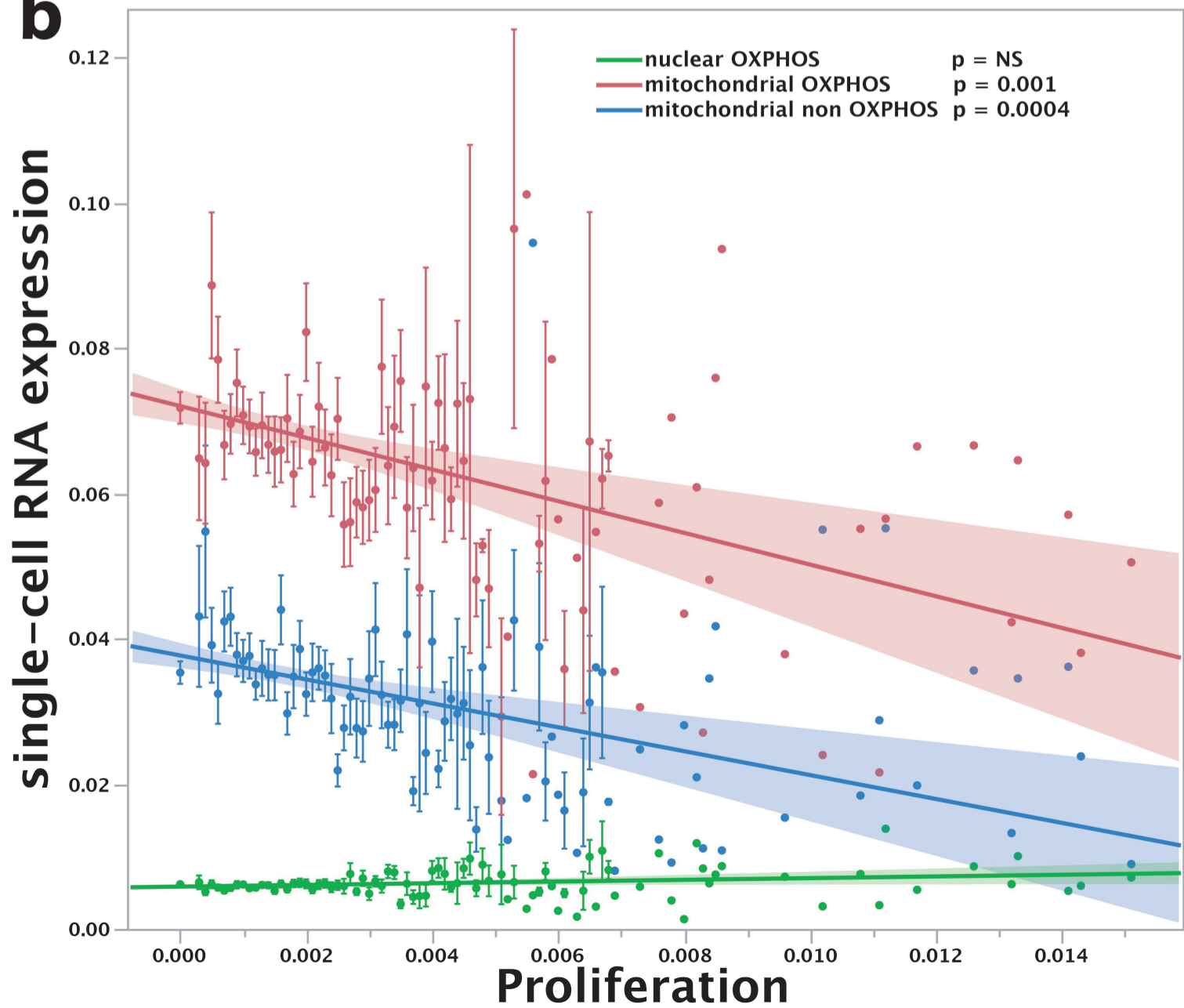
697

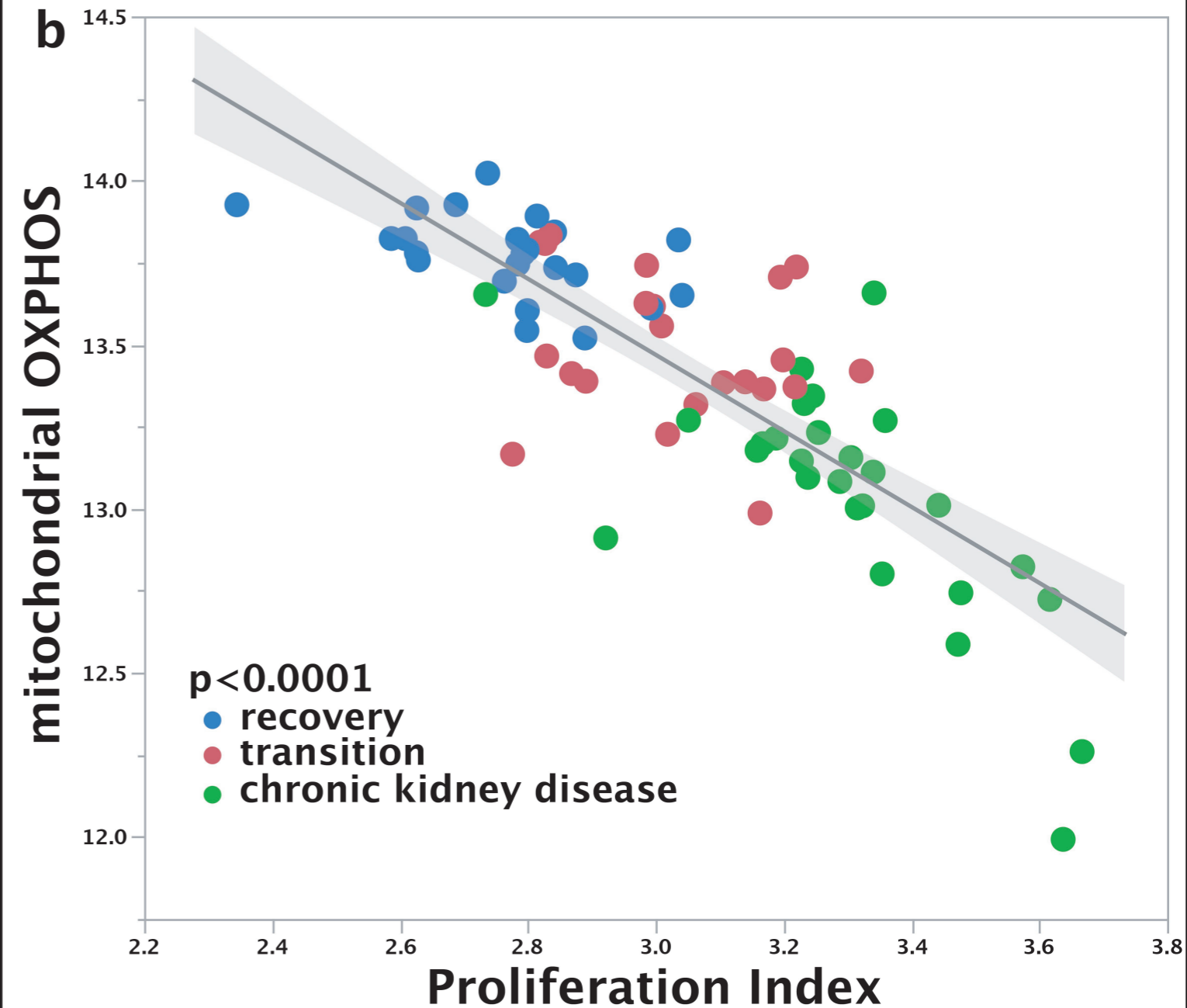
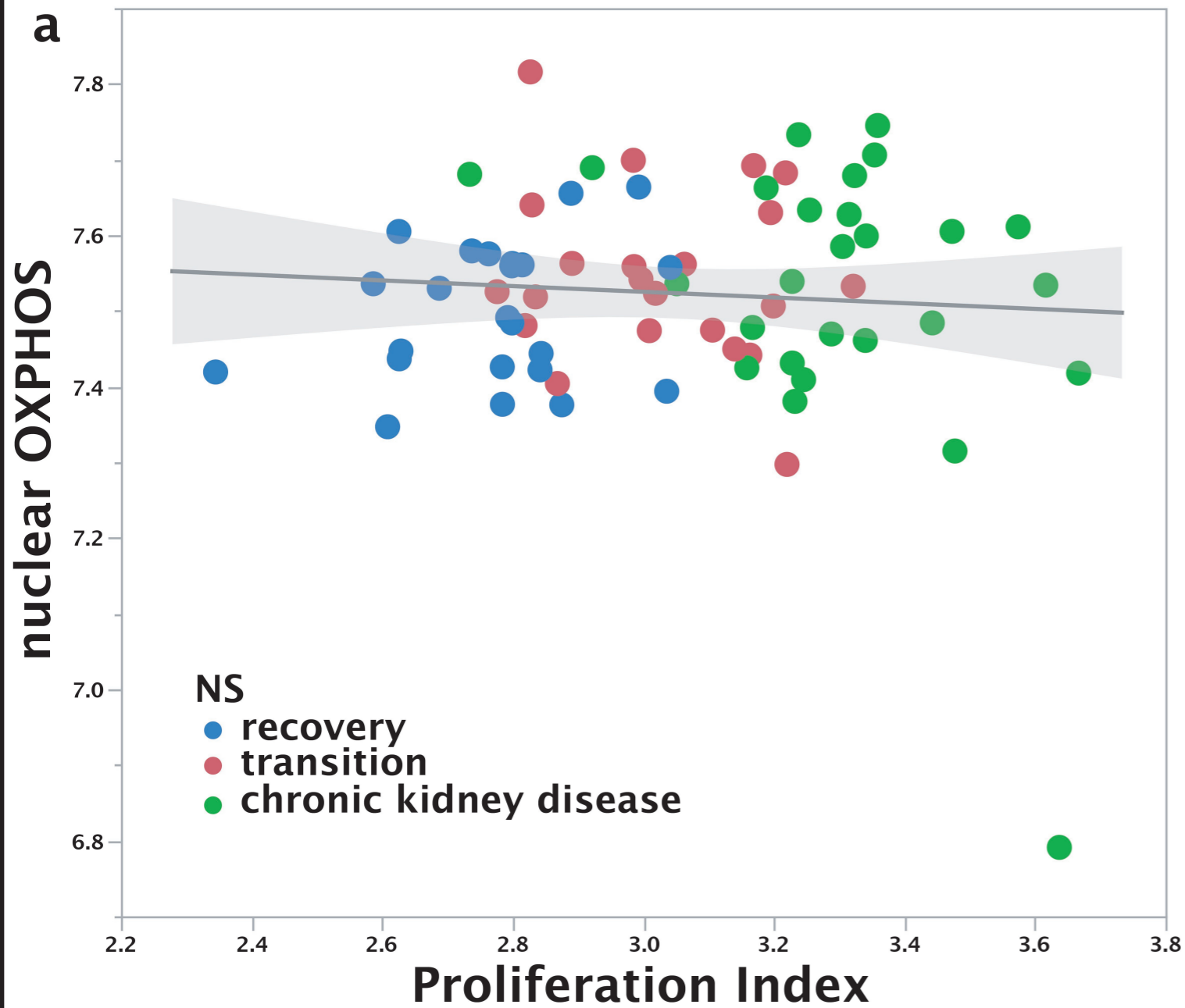
698 **Figure 7.** Impact of energy metabolism changes leading to cellular injury and proliferation in injured
699 kidneys. Top: the lines show the physiological changes in oxidative phosphorylation (pink) and
700 proliferation (blue) leading to full recovery. Bottom: the lines show pathological processes with
701 excessive proliferation leading to cell death by energy depletion (hatched purple area) and persistent
702 oxidative phosphorylation defect leading to chronic kidney disease and fibrosis (hatched green area).
703

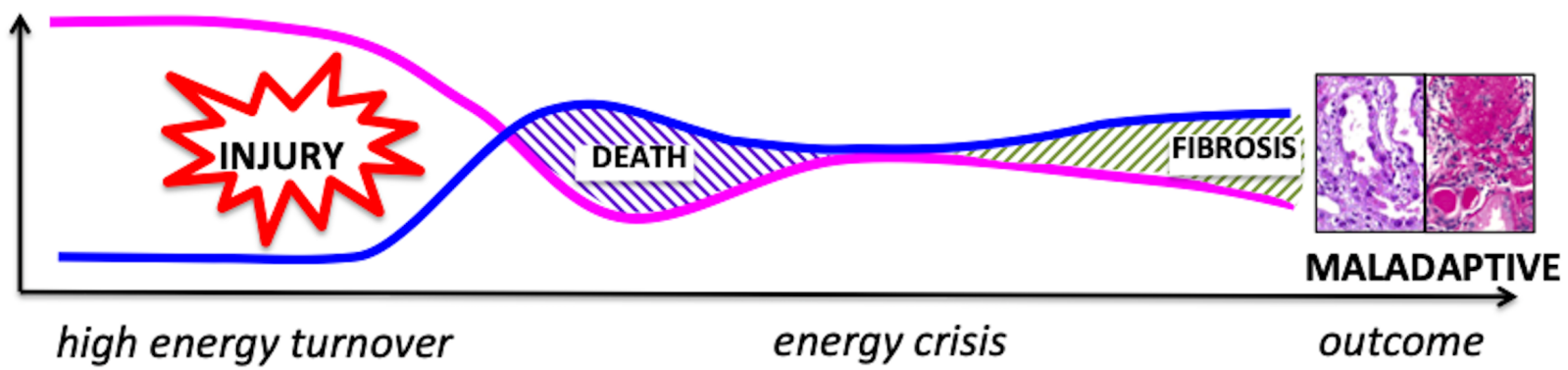
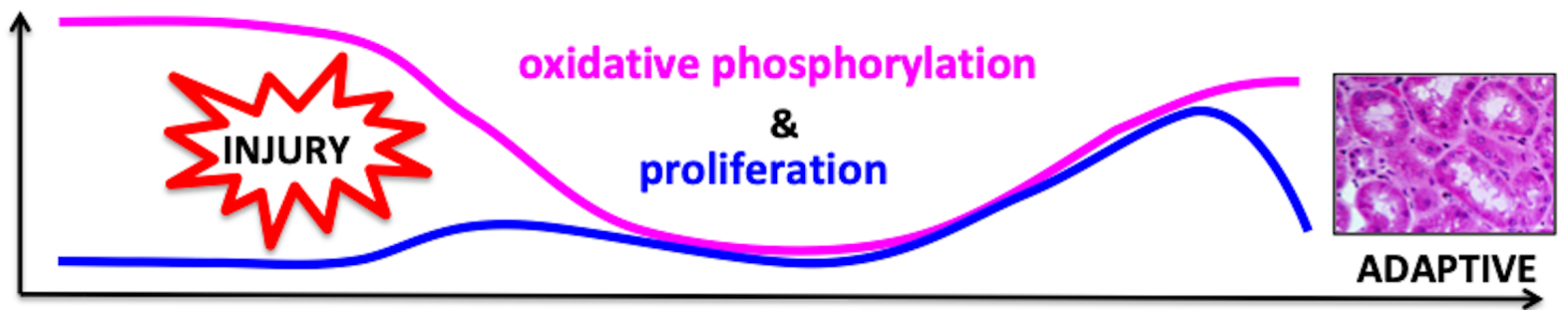






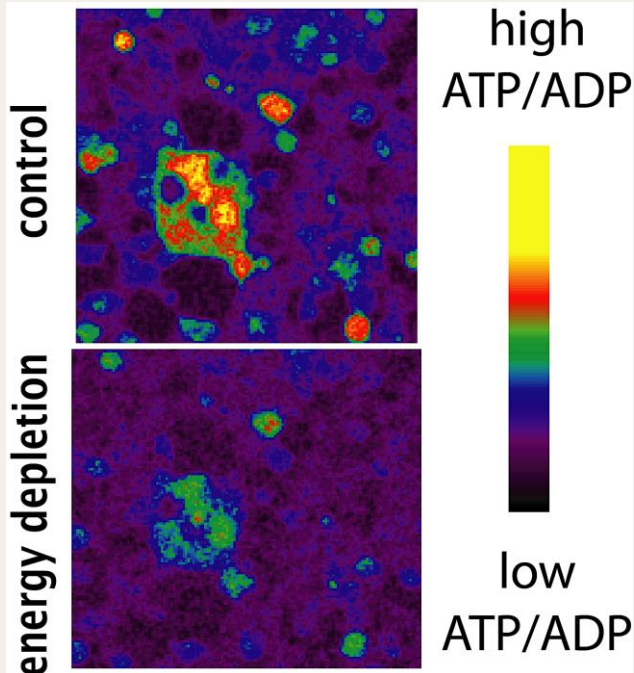
a**b**



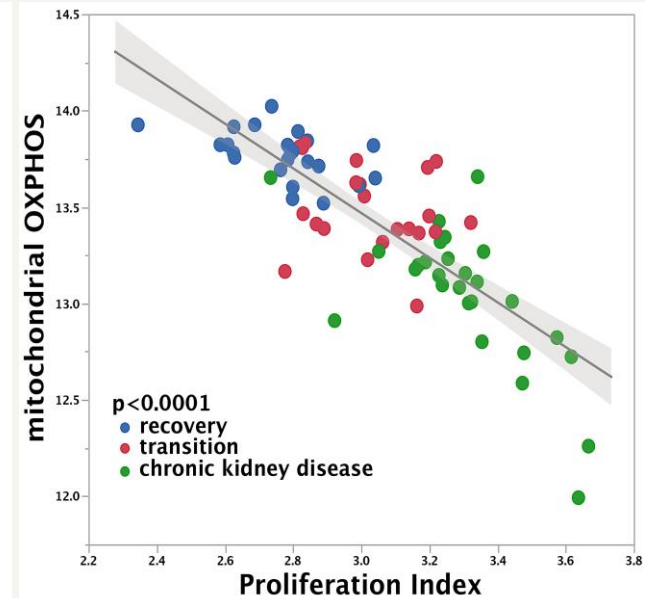
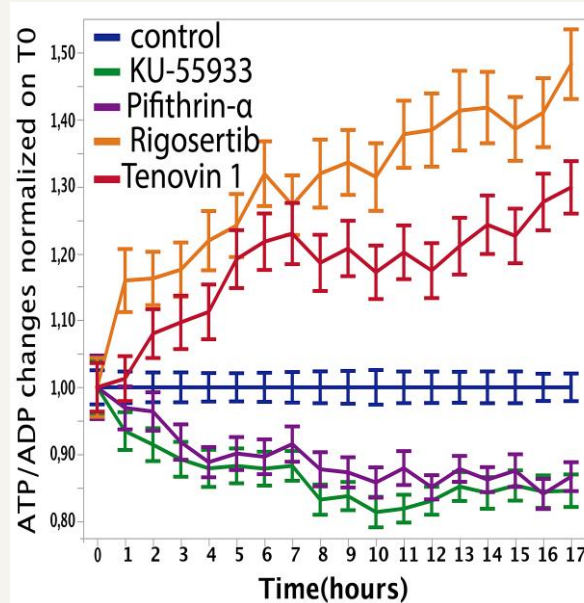


Viability of proliferating kidney cells

METHODS



PROLIFERATION IMPAIRS ENERGETIC STATUS



Proliferation is an energy crisis sensitizing renal epithelial cells to maladaptive repair.